Inorganica Chimica Acta 375 (2011) 150–157

Contents lists available at ScienceDirect

Inorganica Chimica Acta

journal homepage: www.elsevier.com/locate/ica

Synthesis, characterization, crystal structure and antitumor activity of organotin(IV) compounds bearing ferrocenecarboxylic acid

Chengchen Zhu, Liguo Yang, Dacheng Li, Qingfu Zhang *, Jianmin Dou *, Daqi Wang

School of Chemistry and Chemical Engineering, Liaocheng University, Liaocheng 252059, PR China

ARTICLE INFO

Article history:
Received 25 November 2010
Received in revised form 26 April 2011
Accepted 30 April 2011
Available online 11 May 2011

Keywords:
Organotin(IV)
Ferrocenecarboxylic acid
Antitumor activity

ABSTRACT

Four new organotin(IV) complexes $[(Bu_3Sn)(FcCOO)]_n$ (**1**), $[(\mu\text{-}Bu_2Sn)_2(\mu\text{-}Bu_2SnFcCOO)_2(\mu_3\text{-}O)_2(\mu\text{-}OCH_3)_2]_2$ (**2**), $[Ph_3Sn(FcCOO)(H_2O)](phen)$ (**3**) and $[\{Ph_3Sn(FcCOO)\}_2(4,4'\text{-bipy})]$ (**4**) [Fc = $(\eta^5\text{-}C_5H_5)Fe(\eta^5\text{-}C_5H_4)$] have been synthesized and characterized by elemental analyses, IR, (^1H and ^{13}C) NMR spectra and X-ray single-crystal diffraction analyses. The structure analyses show that all tin atoms in complexes **1–4** are five-coordinated with trigonal bipyramid geometry. Complexes **1–4** and FcCOOH undergo reversible one-electron oxidations in methanol solution. The antitumor activities of complexes **1–4** have also been tested. Complexes **1** and **2** exhibit medium activity towards P388 cell lines and Hela cell lines. Complexes **3** and **4** exhibit medium activity towards P388 cell lines but strong activity towards Hela cell lines. This may result from complexes **3** and **4** including the neutral molecules 1,10-phenanthroline and 4,4′-bipy.

1. Introduction

In recent years, organotin(IV) compounds have attracted more attention, not only for their potential antitumour activities [1–10], but also for their versatile structures in solid and solution, such as monomers, dimers, tetramers, oligomeric ladders and hexameric drums and so on [11]. In our previous work, several 12-MC-4 organotin metallacrowns with salicylhydroxamic acid ligand have been successfully designed and prepared [12,13].

Since ferrocene was synthesized by Kealy and Pauson [14], great attention has been paid to the metal complexes containing ferrocenyl ligands. Ferrocenecarboxylic acid is the simplest carboxylic acid containing ferrocene group, It has attracted much attention in the field of coordination chemistry [15] due to its excellent properties such as high thermal stability, excellent redox activity and potential applications in catalysis, magnetism and non-linear optics [16–22]. As a ligand containing typical organometallic group, ferrocenecarboxylic acid has versatile coordination modes, such as monodentate, bidentate bridging, bidentate chelating, and tridentate-bridging (Scheme 1) [23]. Up to now, a large number of transition-metal complexes containing ferrocenecarboxylic acid have been synthesized and characterized [24–30].

However, it is still a big challenge for the preparation of organotin complexes bearing ferrocenecarboxylic groups because of the steric hindrance of ferrocenyl. Till now, only several organotin complexes containing FcCOO group have been structurally characterized by X-ray crystallography, such as $FcCOOSn(CH{=}CH_2)_3$ [31], $[FcCOOSnBu_2O]_2{\cdot}4C_6H_6$ [32], $[n\text{-}BuSnCl(FcCOO)]_3(O)(OH)$ [33], $[\{BuSn(O)\ FcCOO\}_6]$ [34], $\{[\mu\text{-}(n\text{-}Bu)_2Sn(\mu\text{-}FcCOO(n\text{-}Bu)_2Sn(\mu_3\text{-}O)]\text{-}FcCOO\}$[35], $[Me_3Sn(Fc\ COO)]_n$, $[Bn_3Sn(FcCOO)]$, $[BnSn(O)(FcCOO)]_6$, $[Me_2Sn(FcCOO)_2]$ [36], and $[(n\text{-}Bu)_2Sn\ (FcCOO)_2]_2$ [37]. In this report, four new organotin(IV) complexes with ferrocenecarboxylic acid, $[(Bu_3Sn)(FcCOO)]_n$ (**1**), $[(\mu\text{-}Bu_2Sn)_2(\mu\text{-}Bu_2SnFcCOO)_2\ (\mu_3\text{-}O)_2(\mu\text{-}OCH_3)_2]_2$ (**2**), $[Ph_3Sn(FcCOO)(H_2O)](phen)$ (**3**), and $[\{Ph_3Sn(FcCOO)\}_2$ (4,4′-bipy)] (**4**) were successfully prepared and characterized by elementary analyses, FT-IR spectroscopy, NMR spectroscopy and single crystal X-ray diffraction. The in vitro tumor-inhibiting activities of the four complexes against P388 cell lines and Hela cell lines are also investigated.

2. Experimental

2.1. Material and methods

All reagents were obtained from commercially available sources and were used without further purification. IR spectra were recorded on a Nicole-5700 spectrophotometer sodium chloride optics using KBr disks. ^1H and ^{13}C NMR spectra were recorded on Varian Mercury Plus 400 spectrometer operating at 400 and 100.6, respectively. The spectra were acquired at 298 K. ^{13}C spectra are broadband proton decoupled. Elemental analyses were performed with a PE-2400II apparatus.

* Corresponding authors. Tel.: +86 0635 8239298; fax: +86 635 8239001.
E-mail addresses: zhangqingfu@lcu.edu.cn (Q. Zhang), dougroup@163.com (J. Dou).

0020-1693/$ - see front matter Crown Copyright © 2011 Published by Elsevier B.V. All rights reserved.
doi:10.1016/j.ica.2011.04.049

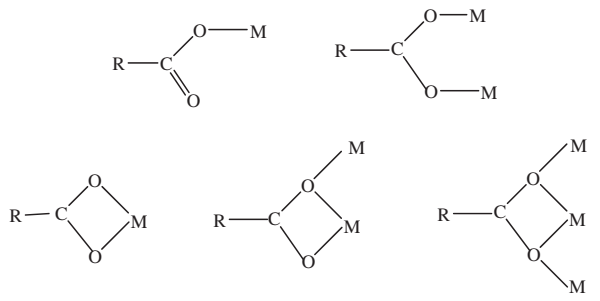

Scheme 1. Typical coordination modes for the ferrocenecarboxylate ligand [R = (η^5-C_5H_5)Fe(η^5-C_5H_4)].

2.2. Syntheses

2.2.1. Preparation of $[(Bu_3Sn)(FcCOO)]_n$ (**1**)

Bu_3SnCl (0.065 g, 0.2 mmol) was added to a solution of FcCOOH (0.046 g, 0.2 mmol) and $(CH_3)_4NOH$ (0.073 g, 0.2 mmol) in methanol (10 mL). The mixture solution was stirred overnight at room temperature in air. Then the above solution was filtered. The filtrate was allowed to stand at room temperature for about three weeks. Finally, red crystal suitable for X-ray diffraction analysis was obtained. Yield: 63 mg (61%). *Anal.* Calc. for $C_{23}H_{36}FeO_2Sn$: C, 53.21; H, 6.99. Found: C, 53.45; H, 6.41%. IR (KBr)/cm^{-1}: 3430(s), 2955(m), 2921(m), 1578(s), 1557(s), 1459(s), 1383(s), 1355(m), 1337(m), 669(m), 603(m), 509(s), 481(m). ^{1}H NMR: δ 0.91–1.67 (m, 54H, *n*-Bu–H), 4.17 (s 10H Cp-H), 4.32 (d 4H Cp-H), 4.76 (d, 4H, Cp-H). ^{13}C NMR: δ 13.66 (CH_3), 26.75, 27.06, 27.38, 27.9, ($SnCH_2CH_2CH_2$), 69.60 (s 10C C_5H_5–C), 70.69 (d 4C C_5H_4–C), 70.75 (d 4C C_5H_4–C), 73.15 (s 2C Cp-C_{ipso}), 176.83, (COO).

2.2.2. Preparation of $[(\mu\text{-}Bu_2Sn)_2(\mu\text{-}Bu_2SnFcCOO)_2(\mu_3\text{-}O)_2(\mu\text{-}OCH_3)_2]_2$ (**2**)

The procedure was the same as that for complex **1**, except that Bu_2SnCl_2 (0.061 g, 0.2 mmol) was used instead of Bu_3SnCl (0.065 g, 0.2 mmol). Yield: 34 mg (46%). *Anal.* Calc. for $C_{56}H_{96}Fe_2O_8Sn_4$: C, 45.32; H, 6.52. Found: C, 45.01; H, 6.85%. IR (KBr)/cm^{-1}: 3373(w), 2956(s), 2857(m), 1580(m), 1463(m), 1381(m), 1332(m), 1180(m), 817(m), 795(m), 681(m), 612(m), 560(m), 483(m). ^{1}H NMR: δ 0.91–1.63 (m, 108H, *n*-Bu–H), 3.48 (s, 12H, CH_3O), 4.17 (s 20H Cp-H), 4.33 (d 8H Cp-H), 4.76 (d, 8H, Cp-H). ^{13}C NMR: δ 13.66 (CH_3), 26.75, 27.06 ($SnCH_2CH_2CH_2$), 27.30, 27.88, ($SnCH_2CH_2CH_2$), 69.60 (s 20C C_5H_5–C), 70.69 (d 8C C_5H_4–C), 70.75 (d 8C C_5H_4–C), 73.13 (s 4C Cp-C_{ipso}), 176.69, (COO).

2.2.3. Preparation of $[Ph_3Sn(FcCOO)(H_2O)](phen)$ (**3**)

Ph_3SnCl (0.077 g, 0.2 mmol) was added to a solution of FcCOOH (0.046 g, 0.2 mmol) and $(CH_3)_4NOH$ (0.073 g, 0.2 mmol) in methanol (10 mL), the mixture solution was stirred 30 min, then 1,10-phen (0.036 g, 0.2 mmol) was added to the solution and stirred overnight at room temperature in air. Then the above solution was filtered. The filtrate was allowed to stand at room temperature for about three weeks. Yellow crystal suitable for X-ray diffraction analysis was obtained. Yield: 105 mg (68%). *Anal.* Calc. for $C_{41}H_{34}FeN_2O_3Sn$: C, 63.35; H, 4.41; N, 3.60. Found: C, 62.57; H, 4.27; N, 3.78%. IR (KBr)/cm^{-1}: 3055(w), 1628(s), 1587(m), 1567(m), 1509(m), 1454(m), 1422(m), 1316(m), 1173(m), 845(m), 732(m), 699(m), 513(m), 485(m), 455(w). ^{1}H NMR: δ 1.87 (s, 2H, H_2O), 3.99 (s 5H Cp-H), 4.34 (d 2H Cp-H) 4.83 (d, 2H, Cp-H), 7.25–8.23, (m, 23H, Ph-H and phen-H). ^{13}C NMR: δ 69.62(s 5C C_5H_5–C), 70.72 (d 2C C_5H_4–C), 70.98 (d 2C C_5H_4–C), 71.27 (s 1C Cp-C_{ipso}), 122.96, 128.50, 128.81, 129.12, 130.02, 136.66, 137.13, 146.21, 150.22, (Ph-C and 1,10′-phen-C), 178.33, (COO).

2.2.4. Preparation of $[\{Ph_3Sn(FcCOO)\}_2(4,4'\text{-bipy})]$ (**4**)

The procedure was the same as that for (**3**), except that 4,4′-bipy (0.016 g, 0.1 mmol) was used instead of 1,10-phen (0.036 g, 0.2 mmol). Yield: 71 mg (54%). *Anal.* Calc. for $C_{68}H_{56}Fe_2N_2O_4Sn_2$: C, 62.14; H, 4.29; N, 2.13. Found: C, 61.54; H, 4.12; N, 2.10%. IR (KBr)/cm^{-1}: 3439(w), 1632(m), 1599(m), 1455(m), 1430(m), 1376(m), 1310(s), 1172(m), 808(m), 783(m), 696(m), 616(m),

Table 1
Crystal, data collection and structure refinement parameters for complexes **1–4**.

	Complex **1**	Complex **2**	Complex **3**	Complex **4**
Empirical formula	$C_{23}H_{36}FeO_2Sn$	$C_{111}H_{190}Fe_4O_{16}Sn_8$	$C_{41}H_{34}FeN_2O_3Sn$	$C_{68}H_{56}Fe_2N_2O_4Sn_2$
Formula weitht	519.06	2953.55	777.24	1314.23
Temperature (K)	298(2)	298(2)	298(2)	298(2)
λ (Å)	0.71073	0.71073	0.71073	0.71073
Crystal system	monoclinic	triclinic	triclinic	triclinic
Space group	$P2(1)/c$	$P\bar{1}$	$P\bar{1}$	$P\bar{1}$
a (Å)	11.9501(17)	11.5591(11)	9.3277(8)	9.7111(7)
b (Å)	10.3200(11)	14.4283(15)	12.1722(12)	9.9415(9)
c (Å)	19.690(2)	20.494(2)	15.5537(16)	16.4615(13)
α (°)	90	91.1800(10)	106.399(2)	82.6450(10)
β (°)	102.640(2)	93.9980(10)	91.4220(10)	84.078(2)
γ (°)	90	102.714(2)	92.3560(10)	65.0790(10)
V (Å^3)	2369.4(5)	3323.8(6)	1691.5(3)	1427.3(2)
Z	4	1	2	1
Absorption coefficient (mm^{-1})	1.680	1.948	1.210	1.414
D_{calc} (mg m^{-3})	1.455	1.476	1.526	1.529
F(0 0 0)	1064	1488	788	662
Crystal size (mm)	0.39 × 0.14 × 0.07	0.46 × 0.44 × 0.43	0.43 × 0.39 × 0.27	0.43 × 0.41 × 0.36
Θ Range (°)	1.75–25.01	1.45–25.02	1.75–25.01	2.27–25.02
Limiting indices	$-14 \leqslant h \leqslant 9$, $-12 \leqslant k \leqslant 12$, $-23 \leqslant l \leqslant 23$	$-13 \leqslant h \leqslant 12$, $-14 \leqslant k \leqslant 17$, $-22 \leqslant l \leqslant 24$	$-11 \leqslant h \leqslant 11$, $-14 \leqslant k \leqslant 11$, $-18 \leqslant l \leqslant 17$	$-11 \leqslant h \leqslant 10$, $-11 \leqslant k \leqslant 11$, $-14 \leqslant l \leqslant 19$
Independent reflection	4123	11 148	8886	7464
Maximum and minimum transmission	0.7519, 0.7192	0.4880, 0.4677	0.7360, 0.6243	0.6300, 0.5815
Goodness-of-fit (GOF) on F^2	1.016	1.029	1.000	1.031
$R[I > 2\sigma(I)]$	R_1 = 0.0670, wR_2 = 0.1664	R_1 = 0.0789, wR_2 = 0.1828	R_1 = 0.0416, wR_2 = 0.0870	R_1 = 0.0603, wR_2 = 0.1344
R (all data)	R_1 = 0.1140, wR_2 = 0.2038	R_1 = 0.1829, wR_2 = 0.2575	R_1 = 0.0683, wR_2 = 0.1030	R_1 = 0.0975, wR_2 = 0.1591
Largest difference in peak and hole ($\times 10^2$ e Å^{-3})	0.993, −0.616	1.135, −0.577	0.848, −0.540	0.913, −0.641

582(w), 510(m), 484(m), 455(m), 448(m). ^{1}H NMR: δ 3.99 (s, 10H, Cp-H), 4.35 (d, 4H, Cp-H), 4.83 (d, 4H, Cp-H), 7.25-8.23, 8.71, 8.73, (m, 38H, Ph-H and 4,4′-bipy-H). ^{13}C NMR: δ 69.66 (s 10C C_5H_5–C), 70.83 (d 4C C_5H_4–C), 71.02 (d 4C C_5H_4–C), 71.29 (s 2C Cp-C_{ipso}), 128–137, (Ph-C), 121.38, 145.54, 150.60, (4,4′-bipy-C), 178.34, (COO).

2.3. X-ray crystallography

Crystal data are given in Table 1, together with refinement details. All X-ray crystallographic data were collected on a Bruker SMART CCD 1000 diffractometer with graphite monochromated Mo Kα radiation (λ = 0.71073 Å) at 298(2) K. A semi-empirical absorption correction was applied to the data. The structure was solved by direct methods using SHELXL-97 and refined against F^2 by full-matrix least squares using SHELXL-97. Hydrogen atoms were placed in calculated positions.

In compound **1**, there are three disordered butyl groups. In the first butyl group, the C13–C15 atoms were distributed two positions with refined site occupancies of 0.724(16) and 0.276(16). In the second butyl group, the C17–C19 atoms were distributed two positions with refined site occupancies of 0.602(12) and 0.398(12). In the third butyl group, the C21–C23 atoms were distributed two positions with refined site occupancies of 0.701(12) and 0.299(12). Similarly, in compound **2**, the disordered butyl carbon atoms C13–C15, C17–C19, C25–C27, C52–C54 and C42 were also distributed two positions with refined site occupancies of 0.60(2) and 0.40(2), 0.629(15) and 0.371(15), 0.458(17) and 0.542(17), 0.396(10) and 0.604(10), 0.52(3) and 0.48(3), respectively. In addition, the DELU and SIMU restraints were applied to C10 and C11 atoms in compound **4**.

2.4. Electrochemistry

Cyclic voltammetry studies were conducted by a potentiostat CHI 1030A (Shanghai Chenhua Instruments Co.). A conventional three-electrode electrochemical system with Ag/AgCl (in 3 M KCl) and a platinum wire (0.5 mm in diameter) were used as the reference and counter electrodes, and a GC as the working electrode, respectively. For CV, the potential were scanned from 0.1 to 1.3 V at a scan rate of 50 mV s^{-1} and the potential referred to the Ag/AgCl. The measurements were performed in CH_3OH solution containing tetrabutyl ammonium perchlorate (n-Bu_4NClO_4) (0.1 mol dm^{-3}) as supporting electrolyte.

2.5. Antitumor activity in vitro

The tumor cell lines which were used for screening were grown and maintained in RPMI-1640 medium supplemented with 10% fetal bovine serum at 37 °C in humidified incubators in an atmosphere of 5% CO_2. Cell proliferation in compound-treated cultures was evaluated by using a system based on the tetrazolium compound (MTT) [38] in the School of Medicine and Pharmacy, Ocean University of China. All cell lines were seeded into 96 well plates at a concentration of about 50,000 cells/mL and were incubated in an atmosphere of 5% CO_2 for 72 h. Then, 150 μL of the sample (organotin complexes) DMSO solution was added and further incubation was carried out at 37 °C for 48 h. The compounds were serially diluted (in four to six steps) with DMSO and added to cell incubation medium at the final concentration of 1.0% DMSO in the medium. Fifty microliters of 0.1% MTT was added to each well. After 4 h incubation, the culture medium was removed, and 150 μL of isopropanol was added to dissolve the insoluble blue formazan precipitates produced by MTT reduction. The plate was shaken for 20 min on a plate shaker to ensure complete dissolution. The optical density of each well was measured at 570 nm wavelength. The antitumor activity was determined three times in independent experiments.

3. Results and discussion

3.1. Syntheses

Complexes **1** and **2** were obtained by the reactions of ferrocenecarboxylic acid with Bu_3SnCl and Bu_2SnCl_2 in methanol solution, respectively. Complexes **3** and **4** were also obtained in methanol solution but using Ph_3SnCl, FcCOOH and neutral ligand 1,10-phenanthroline, 4,4′-bipy as starting materials, respectively. As shown in Scheme 2, all the reactions occurred at the basic conditions.

3.2. IR spectra

The IR spectra of complexes **1–4** were recorded in the range of 4000–400 cm^{-1}. The band at 2955–2852 cm^{-1} for **1**, 2956–2857 cm^{-1} for **2** can be assigned to the sp3 C–H bonds of the butyl groups. The vibrations of Cp-H are much closer to 3100 cm^{-1}. The band at 3055 cm^{-1} for **3**, 3065–2987 cm^{-1} for **4** belongings to C–H vibration of Cp-H and Ph-H from the Ph_3Sn and phen/bpy ligands, overlapping in the spectrum, which agree well with the previous report [27,39]. The strong absorption bands at 1578–1599 and 1383–1422 cm^{-1} ranges can be assigned to the $\nu_{as}(COO^-)$ and $\nu_s(COO^-)$ vibrations. The absorption bands at 1454, 1481 cm^{-1} in complex **3** and 1455, 1479 cm^{-1} in complex **4** can be assigned to C=N vibration [40,41].

3.3. NMR spectra

The ^{1}H NMR spectra show the expected integration and peak multiplicities. The ^{1}H NMR spectra of complexes **1** and **2** show that the chemical shifts of the protons of Cp-ring and butyl bound to tin atom ($CH_3CH_2CH_2CH_2Sn$) exhibit multi signals at the region 4.17–4.76 ppm and 0.91–1.67 ppm and there are no peak of the protons of –COOH, which indicates the oxygen atoms coordinate to the tin atoms. The ^{1}H NMR spectra of complex **2** exhibits a signal peak of the protons of methanol at 3.48 ppm, but no peak exhibits the proton of –OH, which indicates that the methanol was deprotonated. The protons of aromatic rings exhibit at the region of 7.2–8.2 ppm.

In ^{13}C NMR spectra, the positions of Cp-ring signals are almost identical in the four complexes, at the region of 69.6–73.1 ppm. The positions of $CH_3CH_2CH_2CH_2Sn$ in complex **2** is similar to complex **1** and the positions of aromatic ring carbon signals remains almost unchanged in complexes **3** and **4**. The carbon signals of –COO appear at 176.83, 176.69, 178.33, 178.34 ppm in complexes 1–4.

3.4. Electrochemical studies

The electrochemical behaviors of FcCOOH and complexes **1–4** were investigated by cyclic voltammetry. The results were shown in Fig. 1. It can be seen from Fig. 1 that all compounds show a single quasireversible peak with an $E_{1/2}$ value of 0.71 V for FcCOOH, 0.42 V for **1**, 0.45 V for **2**, 0.52 V for **3**, 0.55 V for **4**, respectively. The voltammogram of complexes **1–4** are different from FcCOOH. The half-wave potential of complexes **1–4** is lower than FcCOOH, sugesting that these compounds are easier to undergo sequential oxidation and reduction than FcCOOH. The electrochemical behaviors for complexes **1–4** and ferrocenecarboxylic acid are reversible even after being tested for many cycles. These results suggest that

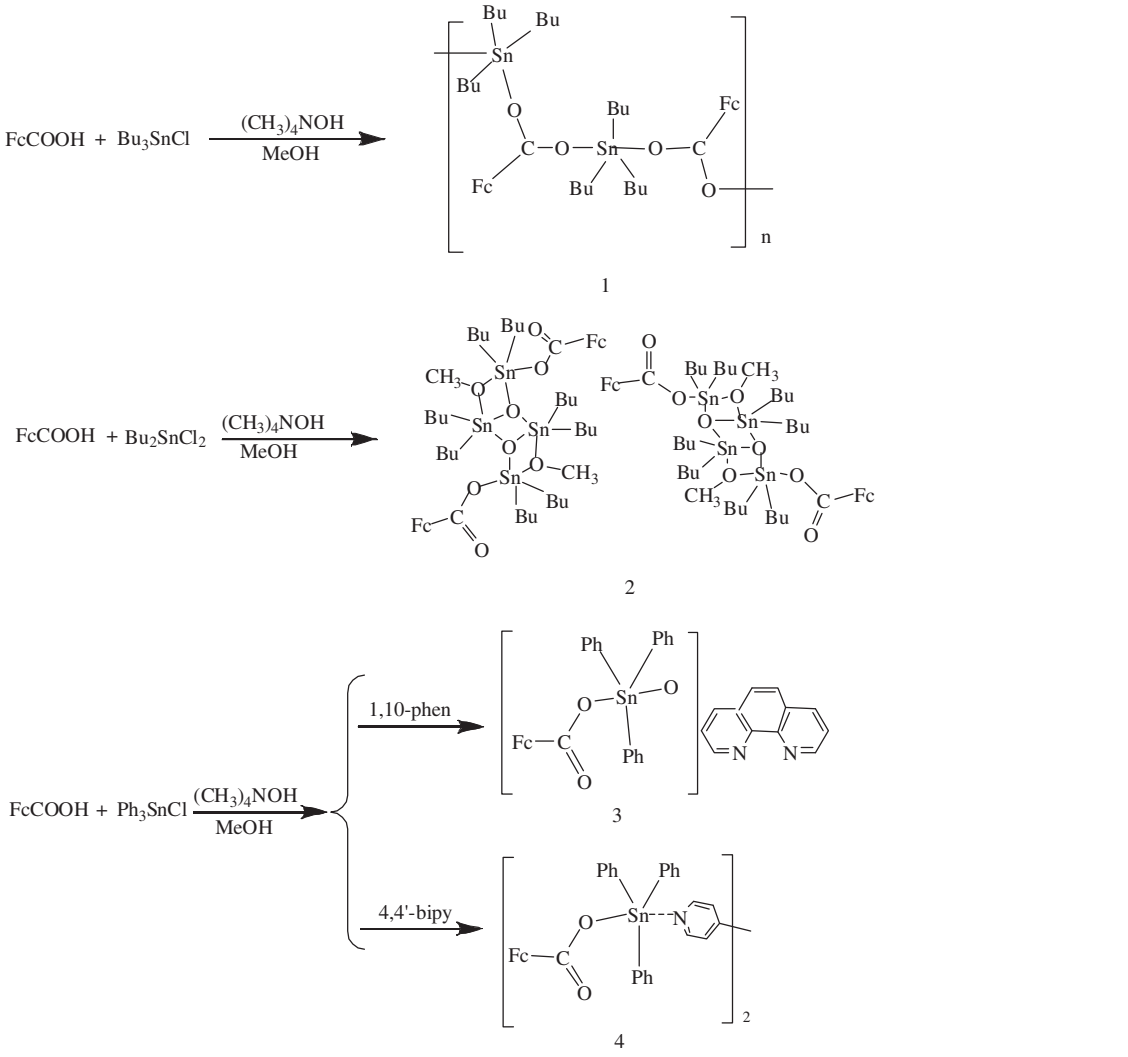

Scheme 2. The syntheses procedures of complexes **1–4**.

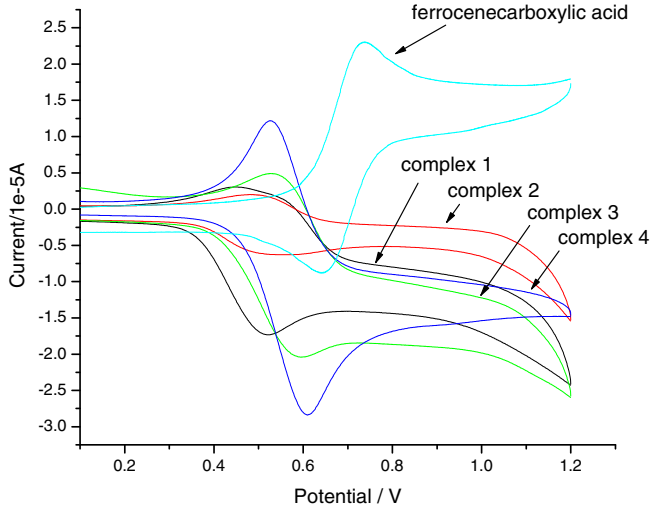

Fig. 1. The cyclic voltammogram of complexes **1–4** and the ferrocenecarboxylic acid in methanol containing *n*-Bu_4NClO_4 (0.1 M) at a scanning rate of 50 mV s^{-1} (vs. Ag/AgCl).

the four complexes are stable and does not decompose upon oxidation, which is consistent with the previous report [34].

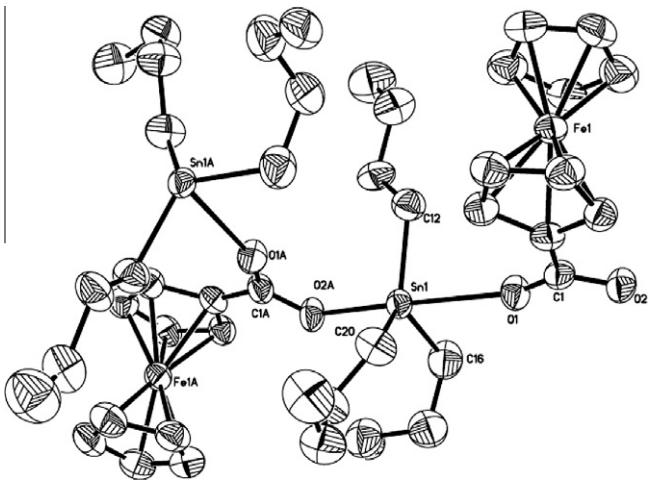

Fig. 2. Molecular structure of the complex **1**.

3.5. Description of crystal structures

3.5.1. Crystal structure of complex (*1*)

The molecular structure of complex **1** is shown in Fig. 2. The selected bond lengths and angles are listed in Table 2. In the

Table 2
Selected bond lengths [Å] and angles [°] for complexes **1**–**4**.

Complex ***1***			
Sn(1)–C(20)	2.063(9)	Sn(1)–O(1)	2.543(6)
Sn(1)–C(12)	2.099(8)	O(1)–C(1)	1.218(8)
Sn(1)–O(2)#1	2.117(6)	O(2)–C(1)	1.265(11)
Sn(1)–C(16)	2.132(11)	O(2)–Sn(1)#2	2.117(6)
C(20)–Sn(1)–C(12)	121.5(4)	C(12)–Sn(1)–O(1)	82.3(3)
C(20)–Sn(1)–O(2)#1	99.1(4)	O(2)#1–Sn(1)–O(1)	174.3(2)
C(12)–Sn(1)–O(2)#1	97.8(3)	C(16)–Sn(1)–O(1)	82.2(3)
C(20)–Sn(1)–C(16)	118.7(5)	O(2)#1–Sn(1)–C(16)	92.6(4)
C(12)–Sn(1)–C(16)	115.8(4)	C(20)–Sn(1)–O(1)	85.5(3)
Complex ***2***			
Sn(1)–O(3)	2.014(8)	Sn(1)–O(1)	2.123(8)
Sn(1)–O(4)#1	2.251(8)	Sn(2)–O(3)#1	2.044(8)
Sn(2)–O(3)	2.127(8)	Sn(2)–O(4)	2.146(8)
Sn(3)–O(7)	2.010(11)	Sn(3)–O(5)	2.128(10)
Sn(3)–O(8)#2	2.273(10)	Sn(4)–O(7)	2.098(11)
Sn(4)–O(7)#2	2.055(10)	Sn(4)–O(8)	2.135(11)
O(1)–C(1)	1.297(15)	O(2)–C(1)	1.293(16)
O(5)–C(28)	1.286(19)	O(6)–C(28)	1.220(18)
O(3)–Sn(1)–O(4)#1	71.4(3)	O(3)–Sn(1)–O(1)	82.0(3)
O(3)#1–Sn(2)–O(3)	73.6(3)	O(1)–Sn(1)–O(4)#1	153.4(3)
O(3)#1–Sn(2)–O(4)	73.1(3)	O(3)–Sn(2)–O(4)	146.7(3)
O(7)–Sn(3)–O(8)#2	70.5(4)	O(7)–Sn(3)–O(5)	81.9(4)
O(7)#2–Sn(4)–O(7)	73.7(5)	O(5)–Sn(3)–O(8)#2	152.3(4)
O(7)–Sn(4)–O(8)	146.2(4)	O(7)#2–Sn(4)–O(8)	72.6(4)
Complex ***3***			
Sn(1)–C(12)	2.126(4)	Sn(1)–C(24)	2.132(4)
Sn(1)–C(18)	2.146(4)	Sn(1)–O(1)	2.152(3)
Sn(1)–O(3)	2.405(3)	O(1)–C(1)	1.280(5)
O(2)–C(1)	1.224(5)		
C(12)–Sn(1)–C(24)	121.91(17)	C(12)–Sn(1)–C(18)	114.47(17)
C(24)–Sn(1)–C(18)	121.65(17)	C(12)–Sn(1)–O(1)	97.93(15)
C(24)–Sn(1)–O(1)	97.77(15)	C(18)–Sn(1)–O(1)	87.97(14)
C(12)–Sn(1)–O(3)	87.14(15)	C(24)–Sn(1)–O(3)	83.97(15)
C(18)–Sn(1)–O(3)	85.02(14)	O(1)–Sn(1)–O(3)	172.60(11)
Complex ***4***			
O(1)–C(1)	1.224(10)	O(2)–C(1)	1.284(10)
Sn(1)–O(2)	2.094(5)	Sn(1)–C(18)	2.106(8)
Sn(1)–C(24)	2.116(8)	Sn(1)–C(12)	2.136(8)
O(2)–Sn(1)–C(18)	101.9(2)	O(2)–Sn(1)–C(24)	95.5(3)
O(2)–Sn(1)–C(12)	91.0(3)	C(18)–Sn(1)–C(24)	128.5(3)
C(18)–Sn(1)–C(12)	114.5(3)	C(24)–Sn(1)–C(12)	113.2(3)

Symmetry transformations used to generate equivalent atoms: (**1**) #1 $-x+2, y+1/2, -z+1/2$ #2 $-x+2, y-1/2, -z+1/2$; (**2**) #1 $-x+1, -y+1, -z$ #2 $-x, -y, -z+1$; (**4**) #1 $-x+1, -y+2, -z$.

crystalline state, this complex adopts an infinite 1D polymeric chain structure. The tin atoms are arranged in zig-zag chain rather than colinear (Fig. 3). And each Sn atom in this complex shows *trans*-trigonal bipyramidal coordination. The three carbon atoms occupy the equatorial positions and the two oxygen atoms occupy the axial positions [O1–Sn1–O2A, 174.3(2)°] for each tin atom. In the complex, FcCOO groups adopt bidentate bridging coordination mode that links the tin atoms into a chain. In addition, the Sn–O bond distances are different [O1–Sn1 2.543(6), O2A–Sn1 2.117(6) Å]. In the carboxylate groups of complex **1**, the C–O bond distances are 1.218(8) and 1.265(10) Å. Therefore, the C–O and C═O can be distinguished according the bond lengths of the Sn–O and C–O, although they are highly delocalized.

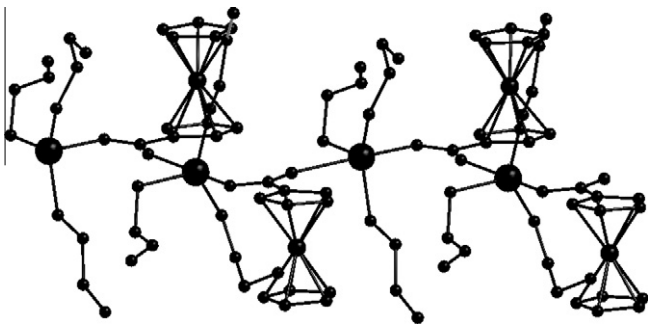

Fig. 3. 1D chain structure of the complex **1**.

3.5.2. Crystal structure of complex (*2*)

The molecular structure of complex **2** is shown in Fig. 4. The selected bond lengths and angles are listed in Table 2. In the crystal structure of complex **2**, there are two molecules in the asymmetric unit. Each unit is a ladder-type structural motif with all tin atoms five coordinated. There was a serious distortion about the coordination geometry of the tin atoms, but it still can be described as a distorted trigonal bipyramidal. In this complex, all FcCOO groups act as monodentate ligand coordinating to tin atoms. The molecule A and B adopt a centrosymmetric dimeric structure by virtue of μ_3-oxo [Sn2–O3 2.127(8) Å, Sn2–O3a 2.044(8) Å; Sn4–O7 2.098(11) Å, Sn4–O7a 2.055(10) Å] which form the central $Bu_4Sn_2O_2$ core with planar Sn_2O_2 ring. There are two tridentate oxygen atoms in each unit which link two endo-cyclic Sn atoms and one exo-cyclic Sn atom. The distance between the two tin atoms is 3.403 Å (Sn1···Sn2, Sn1a···Sn2a) and 3.421 Å (Sn3···Sn4, Sn3a···Sn4a) in the two endo-cyclic. And the distance between the two tin atoms in the exo-cyclic is 3.340 Å (Sn2···Sn2a) and 3.324 Å (Sn4···Sn4a), respectively. The additional links between the endo- and exo-cyclic Sn are provided by bidentate deprotonated methanol that form the asymmetrical bridges (Sn1–O4 2.251(8) Å, Sn2–O4 2.146(8) Å; Sn3–O8 2.273(10) Å, Sn4–O8 2.135(11) Å). The dihedral angle between the planes of the Sn_2O_2 rings is 83.36° in this complex.

In complex **2**, the molecule A and B are linked via C10–H10···O6 interactions. The complex is linked into one-dimensional infinite chains via C10A–H10A···O6A. The oxygen atoms O6 and O6A derive from the carboxyl groups in molecule B. Then the 1D chain is self-assembled into a 2D supramolecular framework (Fig. 5) by C37–H37···O2 interactions. The oxygen atoms O2 and O2A derived from the carboxyl groups in molecule A. The distance of H10···O6 and H10A···O6A is 2.42 Å and the distance of H37···O2 is 2.62 Å, which both lie within the values in previous literature [42,43]. The angle of C10–H10···O6, C10A–H10A···O6A is 169.6° and the angle of C37–H37···O2 is 151.3°. The information hydrogen bonds were showed in Table 3.

3.5.3. Crystal structure of complex (*3*)

The molecular structure of complex **3** is shown in Fig. 6. The selected bond lengths and angles are given in Table 2. For complex **3**, the geometry at Sn1 is distorted trigonal bipyramidal in which the axial apical positions were occupied by two oxygen atoms. The two oxygen atoms come from the water molecular and carboxyl group, respectively. The four atoms Sn1, C12, C18 and C24 which form a palne with the tin atom slightly deviate from the ideal plane by 0.173 Å. The angle of O1–Sn1–O3 is 172.60(11)°. In this complex, ferrocenecarboxylic acid is monodentate ligand and the distance between Sn1 and O1 is 2.152(3) Å. The water molecular is also found in the coordination sphere, with Sn–O bond length is 2.405(3) Å.

As shown in Fig. 7, the adjacent molecules form a linear 1D chain structure by intramolecular C31–H31···O1 and intermolecular C38–H38···O2 hydrogen bonds in which the oxygen atoms O1, O2 derived from the carboxyl group. The distance of C31···O1 and C38···O2 is 3.517(6) and 3.127(7) Å, which both lie within the values in previous literature [44,45]. These adjacent 1D chains are linked into a 2D network via O3–H43···N1 (N atoms derived from 1,10-phenanthroline). The bond distance of H43···N1 is 1.99(2) Å, which is consistent with the values in previous literature [46]. The information hydrogen bonds were showed in Table 3.

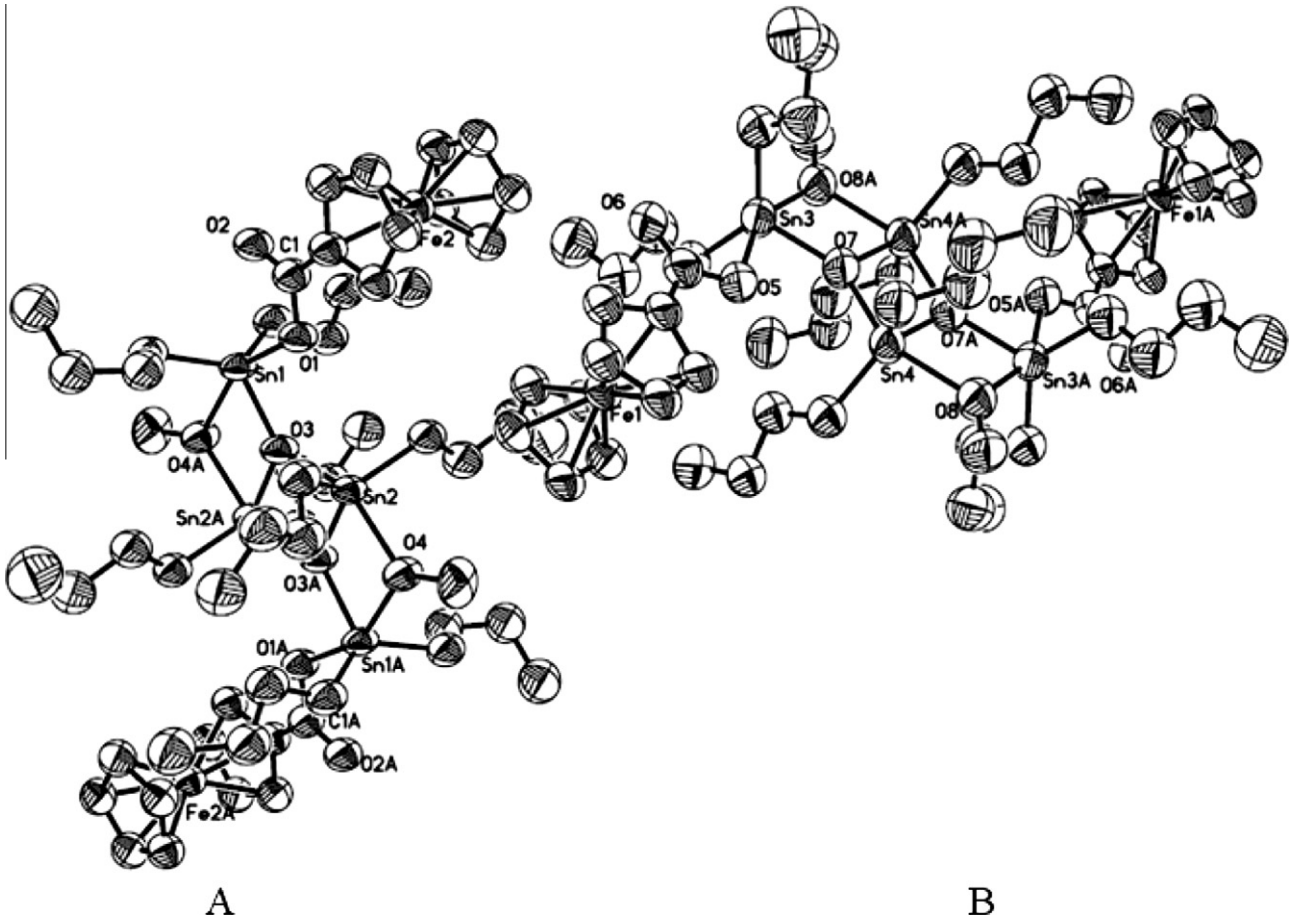

Fig. 4. Crystal structure of the complex **2**.

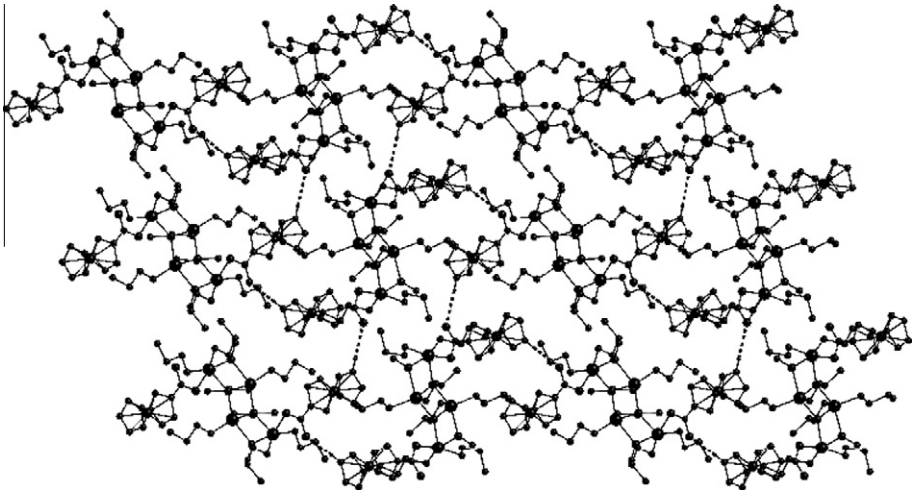

Fig. 5. The 2D network of complex **2**.

*3.5.4. Crystal structure of complex (**4**)*

The molecular structure of complex **4** is shown in Fig. 8. The selected bond lengths and angles are listed in Table 2. For complex **4**, the structure contains two $Ph_3Sn(O_2CFc)$ units associated through a bridging 4,4′-bipy moiety. The geometry of Sn atom is trigonal bipyramidal with a uncoordinated N atom derived of 4,4′-bipy and the angle of O–Sn–N is 175.92°. The distance between Sn and N is 2.722 Å which is close to the Sn–N bond length reported before [47,48]. The three C atoms of phenyl groups form an equatorial plane, and the sum of the trigonal plane angle is 356.06(6)°, while the oxygen atom belonging to the carboxyl groups and the nitrogen atom from 4,4′-bipy occupy the axial apical position.

Table 3
Geometry parameters of hydrogen bonding geometries for the ligand and complexes **2** and **3**.

Complex ***2***				
D–H···A	d(D–H)	d(H···A)	d(D···A)	angle (DHA)
C(10)–H(10)···O(6)	0.98	2.42	3.38(2)	169.6
C(37)–H(37)···O(2)#3	0.98	2.62	3.51(2)	151.3
Complex ***3***				
D–H···A	d(D–H)	d(H···A)	d(D···A)	angle (DHA)
C(38)–H(38)···O(2)#3	0.93	2.27	3.127(7)	153.0
O(3)–H(43)···N(1)#2	0.853(19)	1.99(2)	2.839(5)	175(5)
C(31)–H(31)···O(1)	0.93	2.61	3.517(6)	165.7

Symmetry transformations used to generate equivalent atoms for Complex **2**: #1 $-x+1, -y+1, -z$ #2 $-x, -y, -z+1$ #3 $x-1, y, z$; for complex **3**: #1 $-x+1, -y+1, -z+1$ #2 $x-1, y, z$ #3 $x+1, y+1, z$.

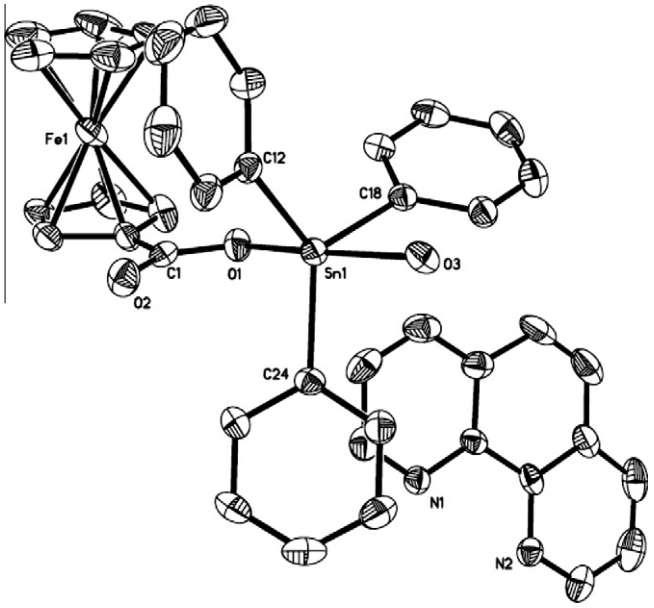

Fig. 6. Crystal structure of the complex **3**.

Being similar to the complexes **2** and **3**, ferrocenecarboxylic acid is also monodentate ligand in this complex and the distance of the Sn1–O2 bond is 2.094(5) Å.

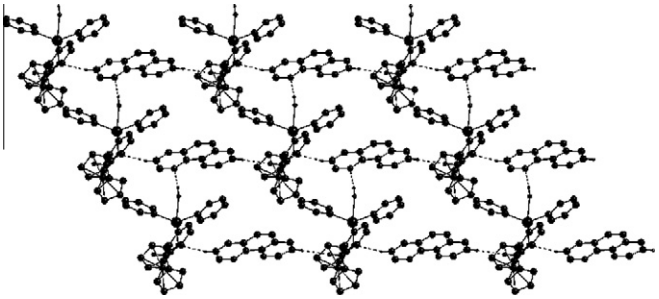

Fig. 7. The 2D network of complex **3**.

3.6. Antitumor activities

Complexes **1–4** were screened for the in vitro tumor-inhibiting activity against P388 cell line and Hela cell line. The inhibitory concentration IC_{50} has been assayed for complexes **1–4**, the corresponding IC_{50} values for P388 and Hela cell lines are listed in Table 4. The results show that complexes **1** and **2** exhibit medium activity towards P388 cell lines and Hela cell lines, complexes **3** and **4** also exhibit medium activity towards P388 cell lines but strong activity towards Hela cell lines, which is more activity than the reported organotin(IV) compounds [12,13,49]. In these four complexes, complexes **3** and **4** more activity than complexes **1** and **2**, which may result from complexes **3** and **4** include the neutral molecules 1,10-phenanthroline and 4,4′-bipy.

4. Conclusion

In conclusion, four new organotin(IV) complexes with ferrocenecarboxylic acid ligand has been successfully synthesized and characterized by elemental analyses, IR, NMR spectra and X-ray single-crystal diffraction. All the tin atoms in complexes **1–4** display five-coordinated trigonal bipyramid geometry. In complexes **2–4**, ferrocenecarboxylate acts as monodentate ligand, while in complex **1** it was a bidentate ligand. Complex **1** is a one-dimensional polymer with the carboxylato groups acting as the bridge to connect the tin units. Complexes **2** and **3** are able to assemble into supramolecular framework through C–H···O and O–H···N weak interactions. Antitumor activities of complexes **1–4** have also been tested. Complexes **1** and **2** exhibit medium activity towards P388

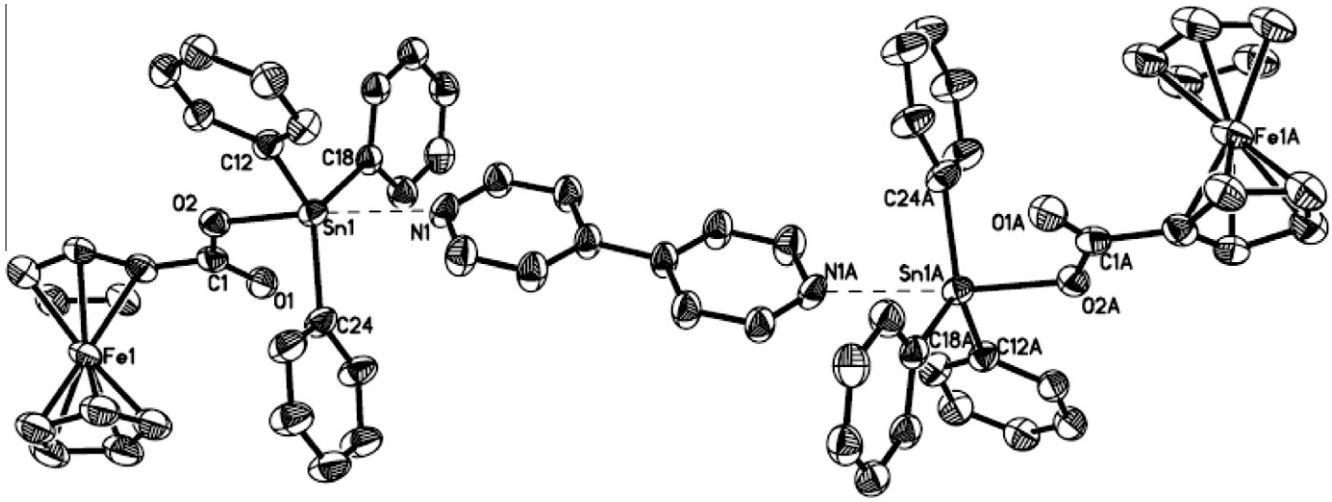

Fig. 8. Crystal structure of the complex **4**.

Table 4
Half maximal inhibitory concentration (IC_{50} μM) of complexes **1**–**4** against tumor cell lines.

Tumor cell line	Complex **1**	Complex **2**	Complex **3**	Complex **4**
Hela	3.56	2.28	0.79	0.65
P388	4.12	3.20	2.44	2.54

$IC_{50} > 1 \times 10^{-4}$ mol/L (inactivity); $IC_{50} \leqslant 1 \times 10^{-4}$ mol/L (weak activity); $IC_{50} \leqslant 1 \times 10^{-5}$ mol/L (medium activity); $IC_{50} \leqslant 1 \times 10^{-6}$ mol/L (strong activity).

cell lines and Hela cell lines, and complexes **3** and **4** exhibit medium activity towards P388 cell lines but strong activity towards Hela cell lines.

Acknowledgments

This work was supported by the National Natural Science Foundation of PRChina (Project No. 20971063, 21001061), Natural Science Foundation of Shandong Province (Y2007B01) and Shandong "Tai-Shan Scholar Research Found".

Appendix A. Supplementary material

CCDC 784813, 784816, 784814, and 784815 contain the supplementary crystallographic data for complexes **1**, **2**, **3**, and **4**, respectively. These data can be obtained free of charge from The Cambridge Crystallographic Data Centre via www.ccdc.cam.ac.uk/data_request/cif. Supplementary data associated with this article can be found, in the online version, at doi:10.1016/j.ica.2011.04.049.

References

[1] C.J. Evans, in: P.J. Smith (Ed.), Chemistry of Tin, Blackie Academic and Professional, London, 1998, p. 442.
[2] S. Durand, K. Sakamoto, T. Fukuyama, A. Orita, J. Otera, Chem. Rev. 93 (1993) 1449.
[3] A. Duthie, D. Dakternieks, M. Schulte, K. Jurkschat, Organometallics 19 (2000) 3220.
[4] A. Orita, Y. Hamada, T. Nakano, S. Toyoshima, Chem. Eur. J. 7 (2001) 3321.
[5] D.P. Miller, P.J. Craig, in: P.J. Smith (Ed.), Chemistry of Tin, Blackie Academic and Professional, London, 1998, p. 541.
[6] L. Pellerito, L. Nagy, Coord. Chem. Rev. 224 (2002) 111.
[7] M. Ashfaq, J. Organomet. Chem. 691 (2006) 1803.
[8] S. Sadiq-ur-Rehman, A. Ali, A. Badshah, E. Malik, G. Ahmed, X. Jin, E.R.T. Tiekink, Appl. Organomet. Chem. 18 (2004) 401.
[9] V. Sharma, R.K. Sharma, R. Bohra, R. Ratnani, V.K. Jain, J.E. Drake, M.B. Hursthouse, M.E. Light, J. Organomet. Chem. 651 (2002) 98.
[10] M. Jain, S. Gaur, S.C. Diwedi, S.C. Joshi, R.V. Singh, A. Bansal, Phosphorus Sulfur 179 (2004) 1517.
[11] R.F. Zhang, Q.F. Wang, M.Q. Yang, Y.R. Wang, C.L. Ma, Polyhedron 27 (2008) 3123.
[12] X.J. Zhao, Q.F. Zhang, D.C. Li, J.M. Dou, D.Q. Wang, J. Organomet. Chem. 695 (2010) 2134.
[13] X.J. Zhao, Q.F. Zhang, D.C. Li, D.Q. Wang, J.M. Dou, Inorg. Chem. Commun. 13 (2010) 346.
[14] T.J. Kealy, P.L. Pauson, Nature 168 (1951) 1039.
[15] D.W. Slocum, C.R. Ernst, Adv. Organomet. Chem. 10 (1972) 79.
[16] Z.L. Chen, Y.S. Ma, F.P. Liang, Z.H. Zhou, J. Organomet. Chem. 693 (2008) 646.
[17] H. Plenio, C. Aberle, Y.A. Shihadeh, J.M. Lloris, R.M. Máñez, T. Pardo, J. Soto, Chem. Eur. J. 7 (2001) 2848.
[18] T. Farrell, T. Meyer-Friedrichsen, M. Malessa, D. Haase, W. Saak, I. Asselberghs, K. Wostyn, K. Clays, A. Persoons, J. Heck, A.R. Manning, J. Chem. Soc., Dalton Trans. (2001) 29.
[19] K.J. Heroux, A.L. Rheingold, D.N. Hendrickson, Eur. J. Inorg. Chem. (2009) 3541.
[20] Z.L. Chen, Y.Y. Ma, F.P. Liang, Z.H. Zhou, Eur. J. Inorg. Chem. (2007) 2040.
[21] A. Togni, T. Hayashi, Ferrocenes: Homogeneous Catalysis, Organic Synthesis, Materials Science, VCH, Weinheim, 1995.
[22] J.S. Miller, A.J. Epstein, W.M. Reiff, Acc. Chem. Res. 21 (1988) 114.
[23] J.M. Dou, Q.L. Guo, L.B. Wu, D.C. Li, D.Q. Wang, H.S. Wang, Y.T. Li, Appl. Organomet. Chem. 20 (2006) 193.
[24] C. Lopez, R. Costa, F. Illas, E. Molins, E. Espinosa, Inorg. Chem. 39 (2000) 4560.
[25] H.J. Kim, W.S. Jeon, J.H. Lim, C.S. Hong, H.J. Kim, Polyhedron 26 (2007) 2517.
[26] A. Bailey, M. Shang, T.P. Fehlner, Inorg. Chem. 39 (2000) 4374.
[27] R. Costa, C. López, E. Molins, E. Espinosa, J. Pérez, J. Chem. Soc., Dalton Trans. (2001) 2833.
[28] C. Lopez, R. Costa, F. Illas, C.D. Graaf, M.M. Turnbull, C.P. Landee, E. Espinosa, I. Mata, J. Chem. Soc., Dalton Trans. (2005) 2322.
[29] R.C. Liu, Y.Q. Ma, L. Yu, J.S. Li, J.R. Cui, R.Q. Wang, Appl. Organomet. Chem. 17 (2003) 662.
[30] J.H. Luo, C.C. Huang, X.H. Huang, J.G. Wang, Acta Crystallogr., Sect. C 64 (2008) m121.
[31] R. Graziani, U. Casellato, G. Plazzogna, J. Organomet. Chem. 187 (1980) 381.
[32] J.X. Tao, W.J. Xiao, Q.C. Yang, J. Organomet. Chem. 531 (1997) 223.
[33] K.C. Kumara Swamy, S. Nagabrahmanandachari, K. Raghuraman, Organomet. Chem. 587 (1999) 132.
[34] V. Chandrasekhar, S. Nagendran, S. Bansal, M.A. Kozee, D.R. Powell, Angew. Chem., Int. Ed. 39 (2000) 1833.
[35] W.G. Lu, J.X. Tao, Z.S. Ma, M. Xiong, Chin. J. Inorg. Chem. 16 (2000) 439.
[36] V. Chandrasekhar, R. Thirumoorthi, Eur. J. Inorg. Chem. (2008) 4578.
[37] W.G. Lu, J.X. Tao, Z.S. Ma, M. Xiong, Y.Z. Wang, Chin. J. Inorg. Chem. 19 (2003) 159.
[38] L.J. Farrugia, J. Appl. Crystallogr. 32 (1999) 837.
[39] X.R. Meng, H.W. Hou, J. Organomet. Chem. 689 (2004) 1218.
[40] G. Marinescu, M. Andruh, M. Julve, F. Lloret, R. Llusar, S. Uriel, J. Vaissermann, Cryst. Growth Des. 5 (2005) 261.
[41] X.R. Meng, B. Xiao, Y.T. Fan, H.W. Hou, G. Li, Inorg. Chim. Acta 357 (2004) 1471.
[42] J.C.M. Rivas, L. Brammer, Coord. Chem. Rev. 183 (1999) 43.
[43] M. Nishio, Cryst. Eng. Commun. 6 (2004) 130.
[44] M.S. Lah, V.L. Pecoraro, Inorg. Chem. 30 (1991) 878.
[45] R. Banerjee, R. Mondal, J.K. Howard, G.R. Desiraju, Cryst. Growth Des. 6 (2006) 999.
[46] A. Jayaraman, V. Balasubramaniam, S. Valiyaveettil, Cryst. Growth Des. 6 (2006) 636.
[47] C.L. Ma, Q.F. Zhang, R.F. Zhang, L.L. Qiu, J. Organomet. Chem. 690 (2005) 3033.
[48] S.A. Bajue, F.B. Bramwell, M. Charles, Inorg. Chim. Acta 197 (1992) 83.
[49] Q.S. Li, M.F.C.G.D. Silva, J.H. Zhao, A.J.L. Pombeiro, J. Organomet. Chem. 689 (2004) 4584.